AD

AD-E403 829

Technical Report ARMET-TR-16024

METHOD FOR DESIGNING ELECTRONIC ASSEMBLIES WITHOUT POTTING FOR GUN LAUNCHED APPLICATIONS THROUGH THE USE OF ADDITIVE MANUFACTURING

Steven Manole
Christopher Stout
Nickolas Baldwin
Richard Granitzki
James Caplinger
Douglas Weinhold
Alfred Rotundo

December 2016

U.S. ARMY ARMAMENT RESEARCH, DEVELOPMENT AND ENGINEERING CENTER

Munitions Engineering Technology Center

Picatinny Arsenal, New Jersey

The views, opinions, and/or findings contained in this report are those of the author(s) and should not be construed as an official Department of the Army position, policy, or decision, unless so designated by other documentation.

The citation in this report of the names of commercial firms or commercially available products or services does not constitute official endorsement by or approval of the U.S. Government.

Destroy by any means possible to prevent disclosure of contents or reconstruction of the document. Do not return to the originator.

REPORT DOCUMENTATION PAGE

Form Approved
OMB No. 0704-01-0188

1. REPORT DATE (DD-MM-YYYY)	2. REPORT TYPE	3. DATES COVERED (*From - To*)
December 2016	Final	May 2013 to June 2015

4. TITLE AND SUBTITLE

METHOD FOR DESIGNING ELECTRONIC ASSEMBLIES WITHOUT POTTING FOR GUN LAUNCHED APPLICATIONS THROUGH THE USE OF ADDITIVE MANUFACTURING

5a. CONTRACT NUMBER

5b. GRANT NUMBER

5c. PROGRAM ELEMENT NUMBER

6. AUTHORS

Steven Manole, Christopher Stout, Nickolas Baldwin, Richard Granitzki, James Caplinger, Douglas Weinhold, and Alfred Rotundo

5d. PROJECT NUMBER

5e. TASK NUMBER

5f. WORK UNIT NUMBER

7. PERFORMING ORGANIZATION NAME(S) AND ADDRESS(ES)

U.S. Army ARDEC, METC
Fuze & Precision Armaments Technology Directorate
(RDAR-MEF-E)
Picatinny Arsenal, NJ 07806-5000

8. PERFORMING ORGANIZATION REPORT NUMBER

9. SPONSORING/MONITORING AGENCY NAME(S) AND ADDRESS(ES)

U.S. Army ARDEC, ESIC
Knowledge & Process Management (RDAR-EIK)
Picatinny Arsenal, NJ 07806-5000

10. SPONSOR/MONITOR'S ACRONYM(S)

11. SPONSOR/MONITOR'S REPORT NUMBER(S)
Technical Report ARMET-TR-16024

12. DISTRIBUTION/AVAILABILITY STATEMENT

Approved for public release; distribution is unlimited.

13. SUPPLEMENTARY NOTES

14. ABSTRACT

A method of using additive manufacturing to print conformal structural supports for printed circuit boards has been shown to be a viable method for ensuring the high G survivability of such electronics in gun launch applications. A novel design, analysis and testing approach has been shown to be successfully demonstrated.

15. SUBJECT TERMS

Additive manufacturing Three-dimensional (3D) print High-G Soft catch (SCAT) gun Guidance electronics On-board recorder (OBR) Precision guided munition (PGM)

16. SECURITY CLASSIFICATION OF:			17. LIMITATION OF ABSTRACT	18. NUMBER OF PAGES	19a. NAME OF RESPONSIBLE PERSON
a. REPORT	b. ABSTRACT	c. THIS PAGE			Chris Stout
U	U	U	SAR	35	19b. TELEPHONE NUMBER (Include area code) (973) 724-5009

Standard Form 298 (Rev. 8/98)
Prescribed by ANSI Std. Z39.18

CONTENTS

FIGURES

FIGURES
(continued)

TABLES

ACKNOWLEDGMENTS

The authors wish to express their gratitude to the following people from the U.S. Army Armament Research, Development and Engineering Center, Picatinny Arsenal, NJ, for supporting this effort: Jin Choi, Patrick Sweeney, and Marvin Heiskanen for overseeing the telemetry system design and data review; Gilmer Vega for his embedded software support; Andy Del Valle and Dave Pritchard for their hard work in assembling the test articles; and Bob Marchak and the soft catch (SCAT) artillery gun team for their testing support.

INTRODUCTION

As precision and smart munitions continue to evolve with electronic technical advances, gun hardening techniques must also keep pace. Traditionally, potting and encapsulating of electronics is a common method for improving their survivability when experiencing a large amount of acceleration. Fully encapsulating the electronics allows them to be fully supported from all sides, as well as performing an environmental dampening function by reducing the stresses on the circuit board and its electronic components (refs. 1 and 2).

While potting is usually an appropriate solution, there are some cases where it is not ideal. In cases with large temperature diurnal cycles over the system's lifecycle, or for components with a high heat source, the rigidity of the potting can cause the components to develop cracks as they try to thermally expand due to differences in the coefficient of thermal expansions between the potting, printed circuit boards (PCB), component mold compound packaging, and solder joints (ref. 3). Also, epoxy-based potting compounds are typically permanent and cannot be removed without damaging the electronics. In cases where removable potting is used, it can be expensive or difficult to remove and replace the potting. If the electronics need to be modified or upgraded, then this can cause issues. In addition, potting is challenging to represent and analyze through modeling and simulation, whereas a simpler solution that could be modeled more quickly and easily would be preferred. Many studies have been conducted to model the effects of potting materials on PCBs and their components: two such studies are provided in references 4 and 5. Both of those studies highlight the importance in developing a modeling and simulation environment that adequately reflects the real world properties of the materials being modeled. Without that, a fully coupled model will not yield useful results.

Haynes, Cordes, et al. (ref. 6) also developed a fully potted electronics model and experimented with a ring potting method as a step away from having potting material fully encapsulate the PCB and its components. Moving one step further toward an alternative to encapsulation is the use of a plastic spacer to provide support between printed circuit boards. The purpose of the spacer is to prevent the boards from deflecting, thus preventing the components on the boards from failing. At the part level, it isn't the individual electrical components that fail under gun launch acceleration loads. An individual component such as a resistor, capacitor, or even a field-programmable gate array on its own is strong enough to survive its own inertial loading due to acceleration. Structural integrity issues arise when the entire PCB is allowed to deflect past the critical strains that solder joints can typically withstand as shown in references 7 and 8. As a rule of thumb, this has been shown to be on the order of 0.004 to 0.005 in. of deflection. An entire PCB effectively deflects like a drum head, causing such failures to occur. Potting solves this deflection issue by uniformly providing a stiffener to the entire PCB, yet introducing the aforementioned thermal cycling issues. The spacers, however, are not permanently attached to the boards, but are instead removable and provide support to the PCB in critical locations. This allows the electronics to be removed or reconfigured if necessary while still providing rigidity in the critical points of the design in order to control overall board deflections. In addition, the spacer does not constrict the components, and only makes contact with areas of the circuit board that can handle being compressed, thus allowing components to expand and contract unconstrained during thermal cycling.

The spacer must fit around the components of the board as not to disturb the circuitry. Therefore, a spacer with the least surface area possible is best, as this will allow for more room to place components. The spacer must prevent the boards from deflecting to the point of component failure. In addition, the spacer must be able to survive the stresses induced during gun launch. A finite element analysis (FEA) can be conducted in order to reduce spacer development costs and time required.

In the development cycle, tests with different spacer designs had to be conducted, which was only feasible in a short time frame using FEA. The output of each analysis contained displacement data at each node of the model. By comparing two data points on the surface of the board, the team was able to determine axial deflection of the modelled PCB across the connecting line. This can be done across any component on the board to determine the deflection of that specific component. The deflection of the entire board can be determined by subtracting the minimum displacement of the board from the maximum displacement.

METHOD

Overview

The focus of this analysis was on the printed circuit board deflection and, thus, the displacement data at each node was documented. In addition, the stress at each node was calculated using material properties.

Initial Method – On-board Recorder

The software used to run the FEA was ABAQUS/Explicit. This package was chosen for its maturity in handling high dynamic events. In addition, it was able to handle the large analysis that was necessary, with up to 671,687 elements for the most complex model.

The initial configuration modeled was that of a U.S. Army Armament Research, Development and Engineering Center (ARDEC), Picatinny Arsenal, NJ telemeter ARRT - 158 ARDEC on-board recorder (OBR). The OBRs are commonly used during high-G (G-force) testing to measure and record in-bore accelerations seen by test projectiles. High-frequency, high-G accelerometers are used to quantify the gun launch environments (ref. 9) and/or in-flight dynamics, as well as serve as an acceleration environment recorder for other ride-along component qualification. The OBR was selected as the initial method because of its ability to provide validation testing of the spacer-supported PCBs alongside a nearly identical potted OBR system. Two general models were used for this analysis. One was a reduced model that included only the spacers and PCBs, including a rigid body against which the top spacer was placed. This model ran very quickly and could be used to test spacer designs at a very quick pace to determine whether or not they were feasible. A full model was also run that included the entire projectile assembly. This model took much longer to run and was only used to verify spacer designs once they had been refined using the reduced model.

The FEA was performed in two steps. The first step was to apply the initial conditions and boundary conditions. The second step was to apply the load based upon an acceleration profile. The load was applied over the full 0.016 sec of the second step.

Initial Method - Modeling Assumptions

The criterion for failure of this analysis was a board deflection of greater than 0.005 in. This was refined further into the modeling process as a deflection across a single component of greater than 0.005 in. Refinement occurred when using the full model that included the board components. It is assumed that the components will function as long as they do not exceed this prescribed amount of deflection at any point during gun launch (ref. 10). The details of the individual solder joints, however, were not modeled. Components were only tied to the PCB.

Initial Method - Parts, Instances, and Simplifications in the Model

The geometry of the spacers and circuit boards were exported as a STEP (*.stp) file from the Pro-Engineer computer-aided design (CAD) model and imported into ABAQUS computer-aided engineering (CAE). As described later in this section, the spacer design evolved through multiple iterations, and each was imported and meshed. In order to reduce complexity, and thus, the run time of the model, the geometry of the board components was simplified. This simplification preserved their mass, but not their exact geometry, as the weight of the components is what contributes to the board deflection. This was done by smearing the total component weight across the density of the PCB. In addition, the model of the spacer was very simple and did not include a method for being attached to the assembly, so a tie constraint was used instead for this purpose.

The full model used in the FEA included two spacers to keep the circuit boards from deflecting, as seen in figure 1. This modeled the entire projectile assembly to check that the stresses transmitted through the assembly were similar to those experienced by the reduced model and to further validate the results.

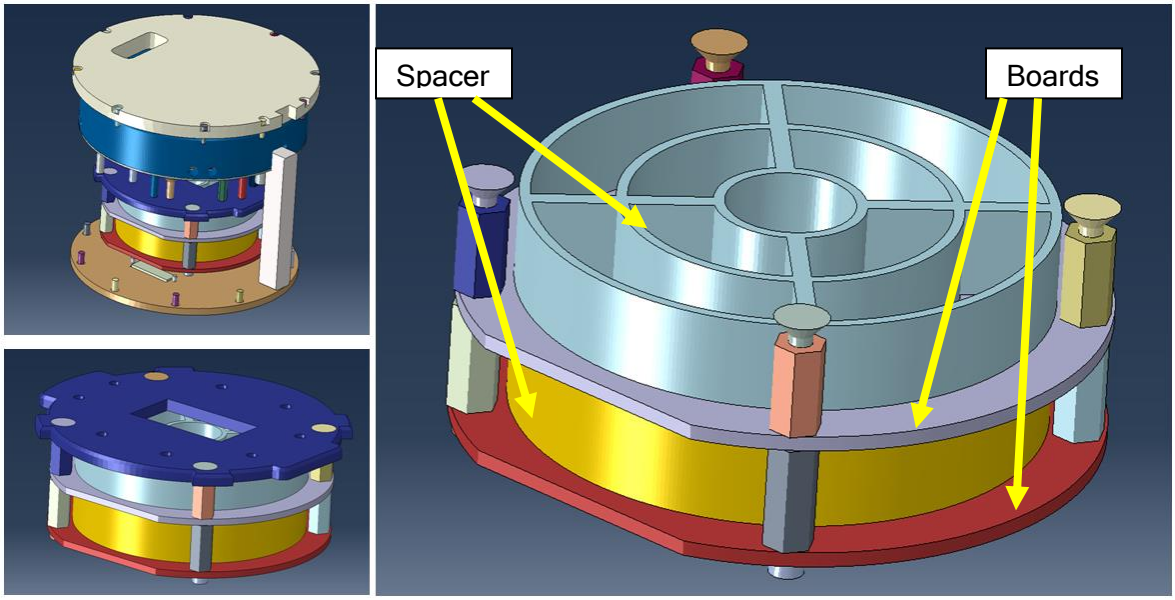

Figure 1
Closeup of spacer and board assembly within full model

Initial Method - Material

All materials used in the reduced model analysis are listed in table 1. There were more materials and parts used in the full analysis; however, the parts that are independent of the spacer and board assembly are not listed. Figure 2 shows the materials of the parts in the reduced model. The materials described in table 2 for the reduced model are the same for the corresponding parts of the full model. For the plastic components, experimental data was used to roughly fit a Johnson-Cook constitutive model in a similar manner as done by Stout et al. (ref. 11). Although not all that well suited for capturing the material behavior far into the damage region, it does adequately capture the nonlinearities seen just after yielding in such reinforced polymers.

Table 1
Materials and material properties

Material name	Material model	Young's modulus (psi)	Poisson's ratio	Density (lbm/in.^3)
FR4	Johnson-Cook	3600000	0.136	0.794
Polycarbonate (Lexan)	Johnson-Cook	350000	0.37	0.0428
AL7075-T6	Johnson-Cook	10300000	0.33	0.101
Ceramic_X7R_Paper	Johnson-Cook	15200000	0.3	0.214

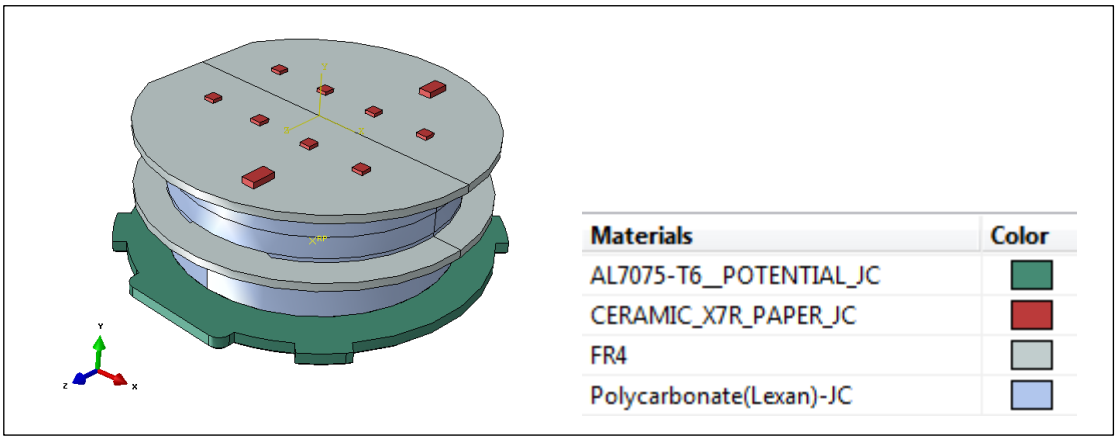

Figure 2
Materials in reduced model

Table 2
Bill of materials for spacer and board assembly

Part name	Material
spacer	Polycarbonate (Lexan)
spacer-digital-bot	Polycarbonate (Lexan)
analog-board-minimal	FR4
digital-board-minimal	FR4
regboard	AL7075-T6
(all board components)	Ceramic_X7R_Paper

Initial Method - Finite Element Mesh

There were 348,648 total elements and 450,353 total nodes for the reduced model with the final spacer design. There were 671,687 total elements and 920,832 total nodes for the full model with the final spacer design. These node and element counts are of similar magnitude for all the spacer revisions. Figure 3 shows the mesh for the full model. This mesh is shown in more detail for the inside of the projectile assembly in figure 4. All parts in the reduced model are listed with their corresponding number of elements and nodes in table 3. The additional parts in the full model are not listed. The meshed reduced model in figure 5 shows most of these parts. The parts that are hidden are PCB components obscured by the spacer.

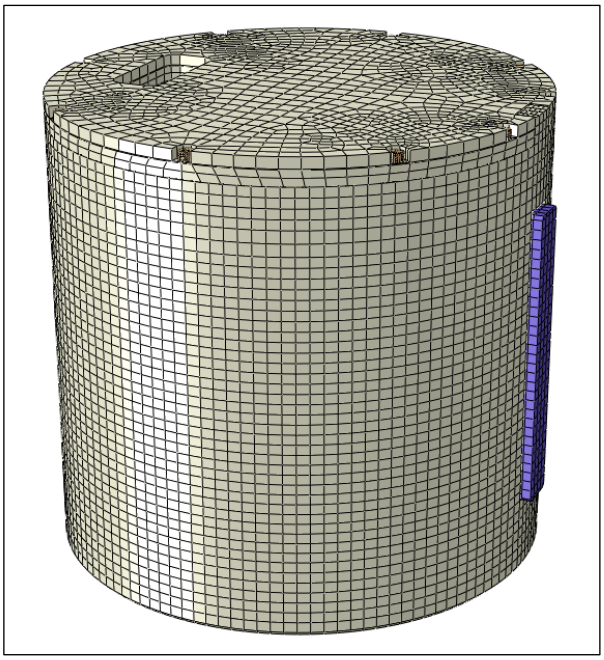

Figure 3
Meshed full model

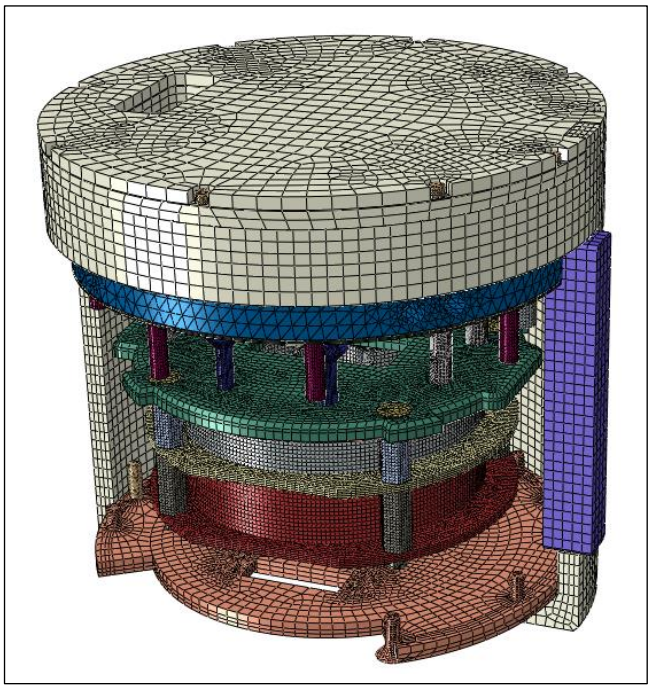

Figure 4
Meshed full model showing spacer and board assembly

Table 3
Mesh properties of each part in reduced model

Model part name	Element type	Elements	Nodes
analog-board-minimal_asm-1	C3D8R	84768	107155
analog-board-minimal_asm-2	C3D8R	50	132
analog-board-minimal_asm-11	C3D8R	50	132
analog-board-minimal_asm-12	C3D8R	16	50
analog-board-minimal_asm-20	C3D8R	36	84
digital-board-minimal_asm-1	C3D8R	84768	107155
digital-board-minimal_asm-6	C3D8R	50	132
digital-board-minimal_asm-9	C3D8R	196	450
digital-board-minimal_asm-48	C3D8R	90	220
digital-board-minimal_asm-50	C3D8R	90	220
digital-board-minimal_asm-55	C3D8R	16	45
digital-board-minimal_asm-58	C3D8R	144	252
digital-board-minimal_asm-59	C3D8R	49	128
gswitch_mass_equiv	C3D8R	1000	1331
regboard	C3D8R	52060	65975
spacer_rev21	C3D8R	65085	86526
spacer-digital-bot_rev6	C3D8R	59092	77556

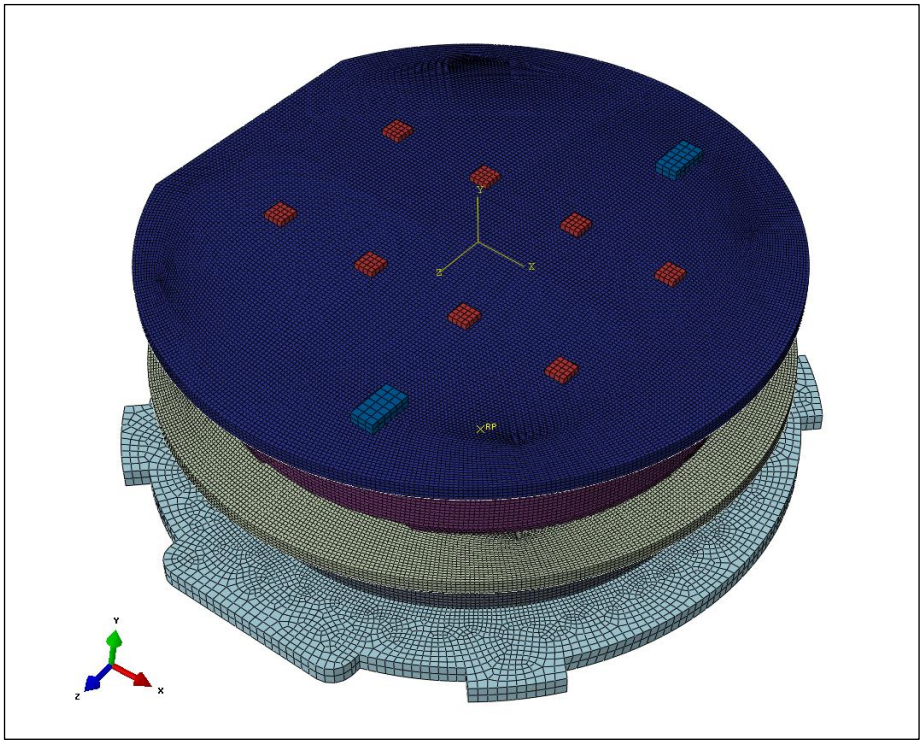

Figure 5
Meshed reduced model

Initial Method - Interaction and Constraints

There were seven tie constraints placed on the model. Three tie constraints were used to tie the components to the boards. Four tie constraints were used to tie the spacers to the boards. All interactions are highlighted in figure 6. The regulation board at the bottom of the figure is treated as a

rigid body for the reduced model analysis. This aluminum part is thicker than the PCBs and deformed very little relative to the rest of the assembly in preliminary runs. By making this part rigid, the speed of the analysis was improved without much impact on the results.

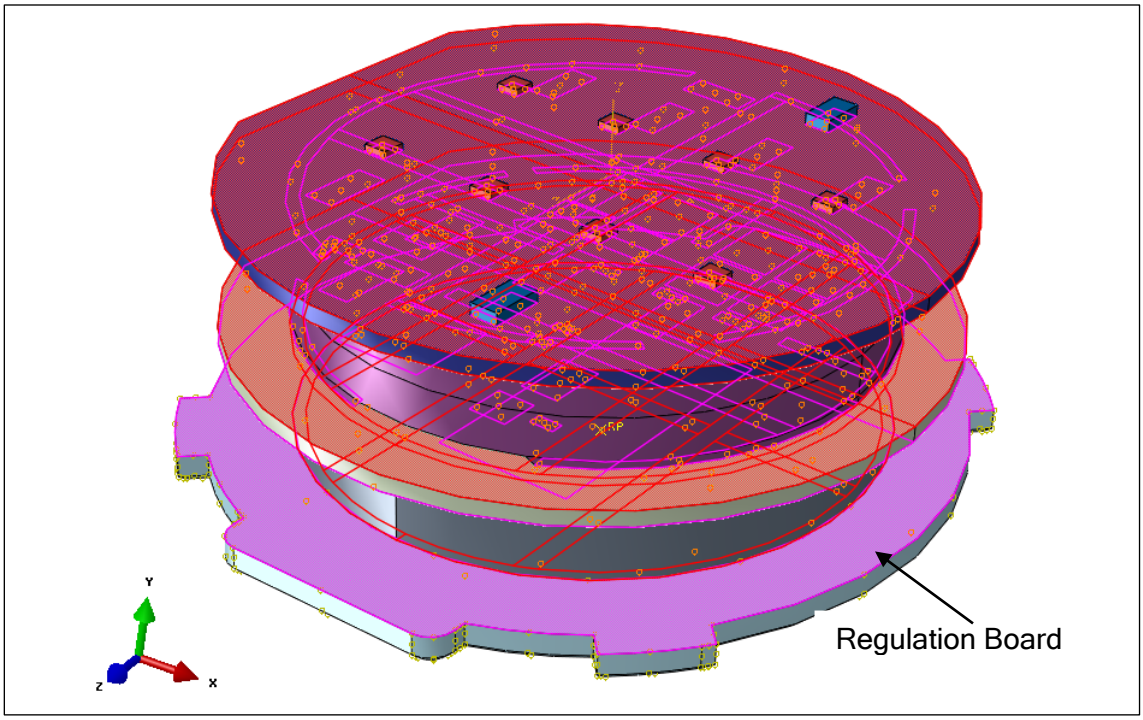

Figure 6
Interactions in reduced model

Initial Method - Boundary Conditions

The reduced model had boundary conditions applied to only allow for translation in the y-direction and rotation about the y-axis. The full model did not have any fixed boundary conditions. These boundary conditions can be seen applied to the nodes with blue and orange arrows in figure 7.

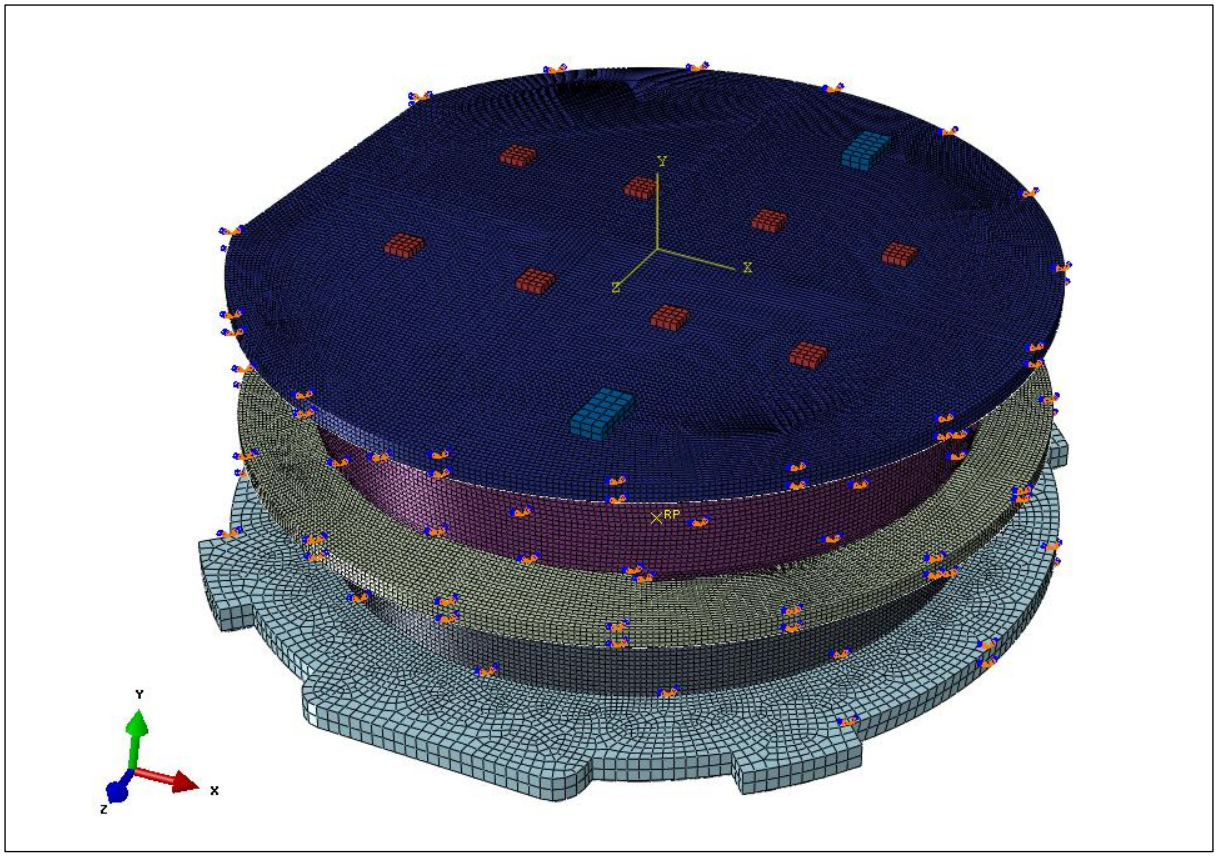

Figure 7
Boundary conditions on reduced model

Initial Method – Loads

An acceleration boundary condition served as the load for this model. It was applied at the reference point on the rigid body in the reduced model and at the base of the projectile in the full model. The reduced model ramped up to 17,000 gs of acceleration, chosen to be about 25% greater than the maximum expected during setback. The full model used an acceleration profile based on actual recorded data. The acceleration profile for the full model is provided in figure 8. In addition to the axial acceleration, there was also balloting in the x- and z- directions. These loads can be seen on the full model in figure 9. Figure 10 shows the acceleration placed on the reference point in the reduced model.

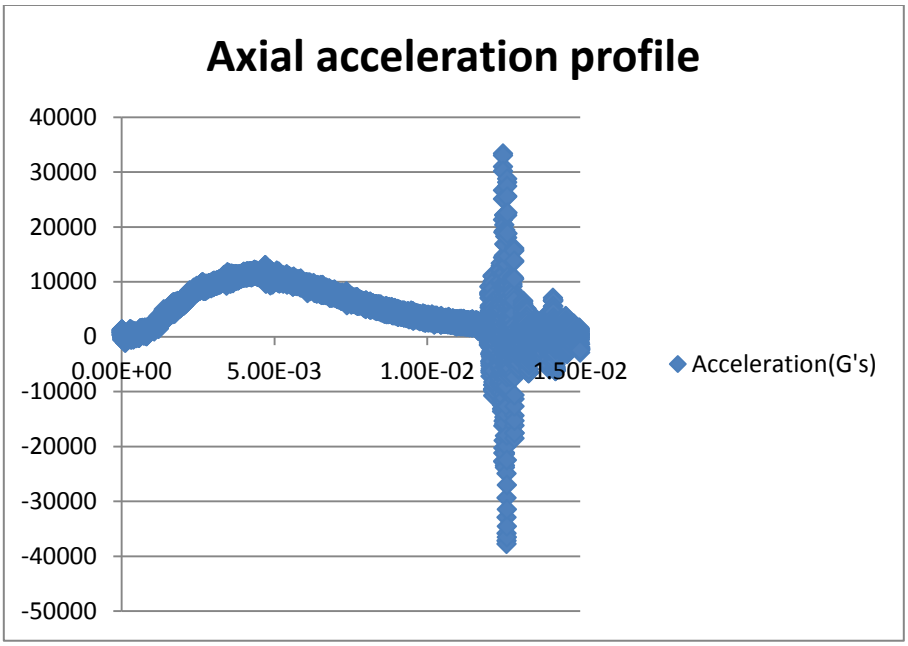

Figure 8
Acceleration profile used for full model

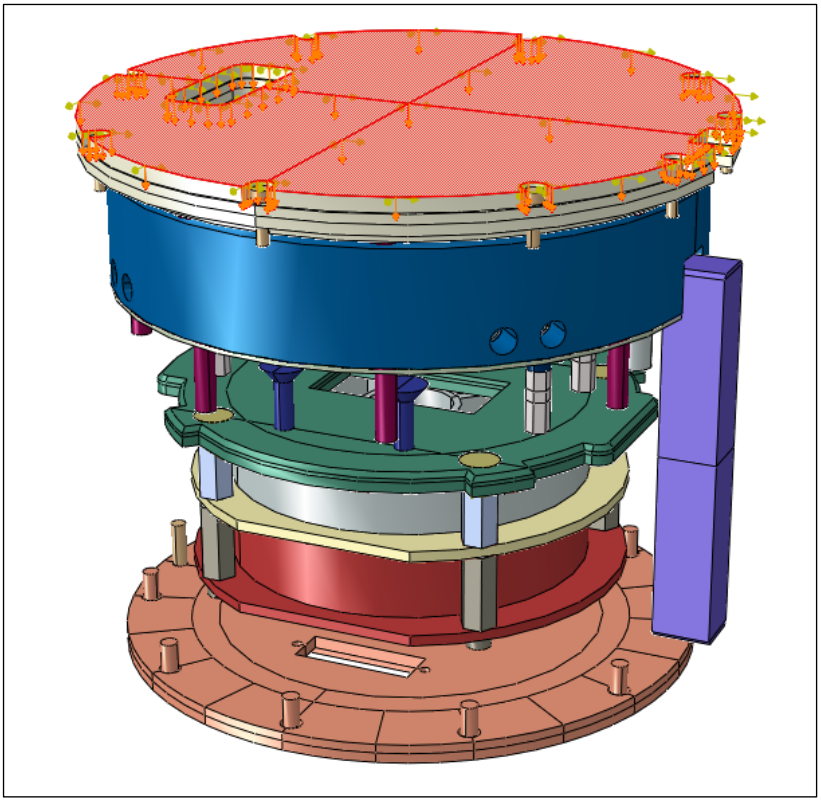

Figure 9
Load applied to full model

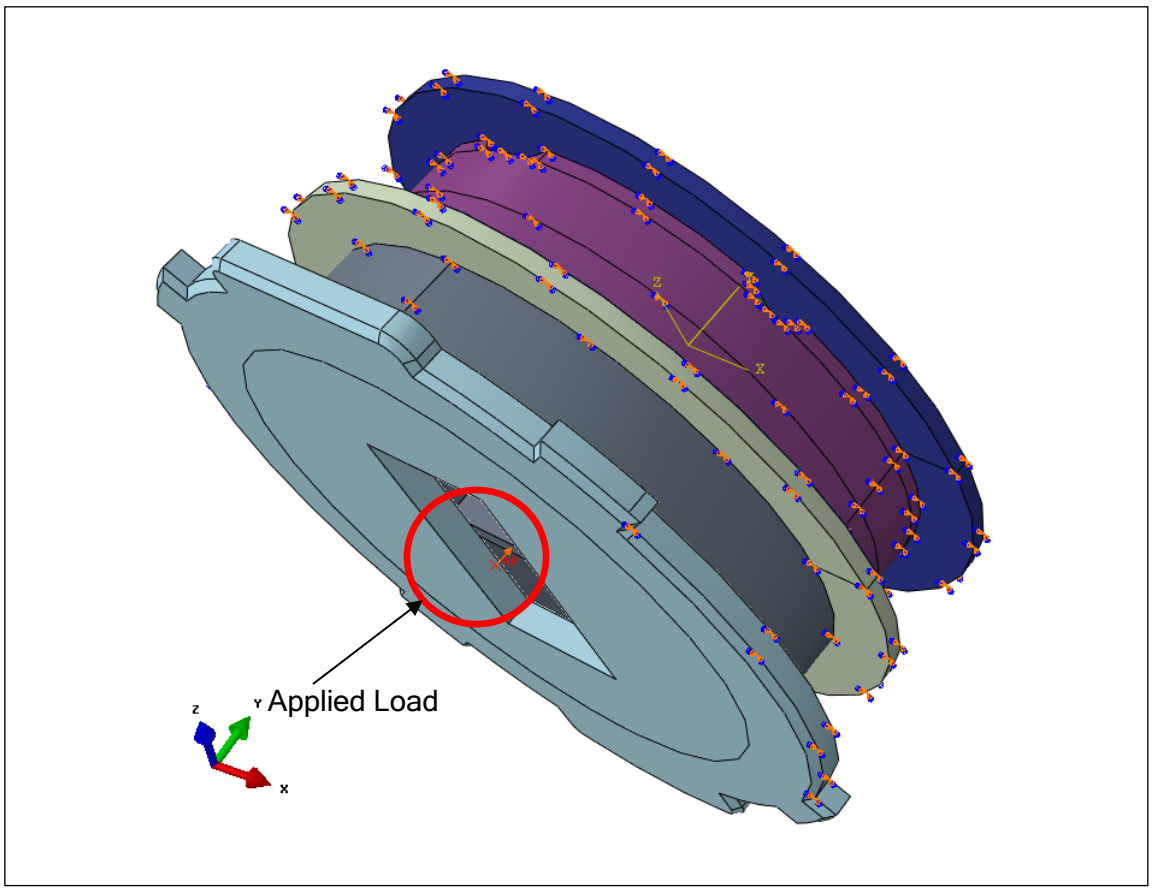

Figure 10
Load applied to reduced model

Initial Method - Results

For each of 20 equal time intervals, the displacement of every node was saved to the results file. These results could be visualized in such a way to identify the interval in which the board experienced the greatest deflection. By manipulating the results display, one could create a visualization that shows whether or not a component was experiencing more than the 0.005 in. deflection required for failure, as described in the modeling assumptions.

There was an initial test done to determine the viability of possible materials for the spacer. The two materials that were tested were nylon and polycarbonate. For this test, the model consisted of a single spacer between two empty circuit boards to which a load of 8000 gs was applied. The nylon spacer was crushed between the two circuit boards. The polycarbonate spacer survived with very little strain (0.099% where 7% could indicate failure). Both of these results are shown in figure 11. The remaining spacer designs all use polycarbonate for the material since this material performed very well in the analysis.

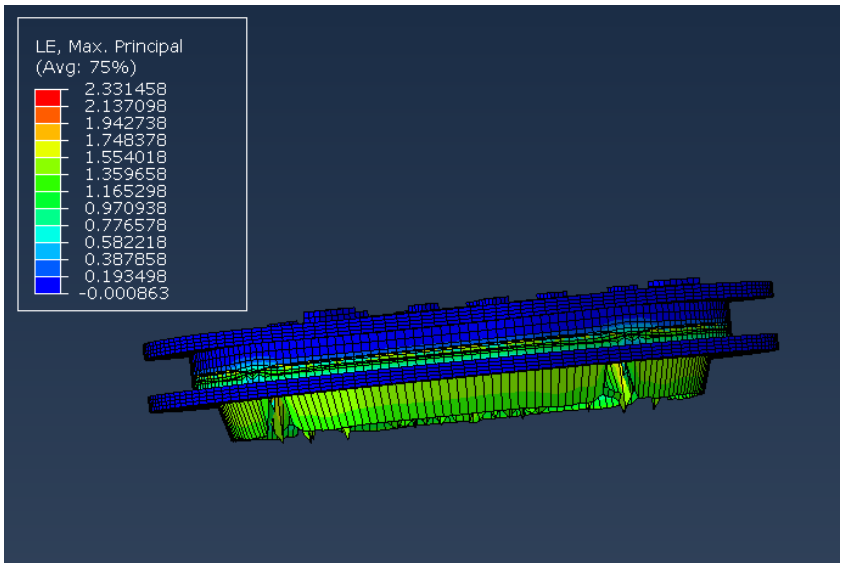

(a)
Nylon

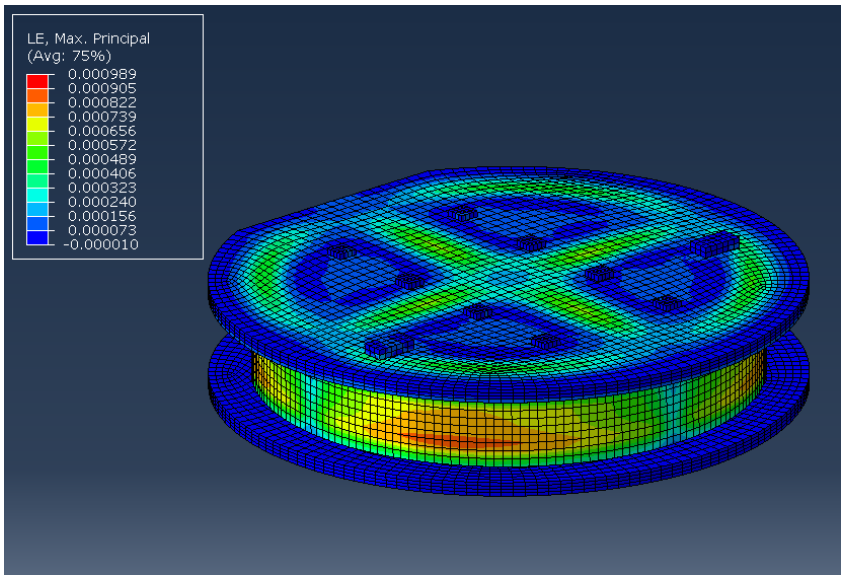

(b)
Polycarbonate

Figure 11
Results of testing done to determine the viability of possible materials for the spacer

There were 21 revisions of the spacer design tested in the reduced model. Seven of these revisions were tested in the full model as well. The final revision was tested only in the full model. All 22 revisions of the spacer design are included in figure 12 (in order from left to right, and top to bottom).

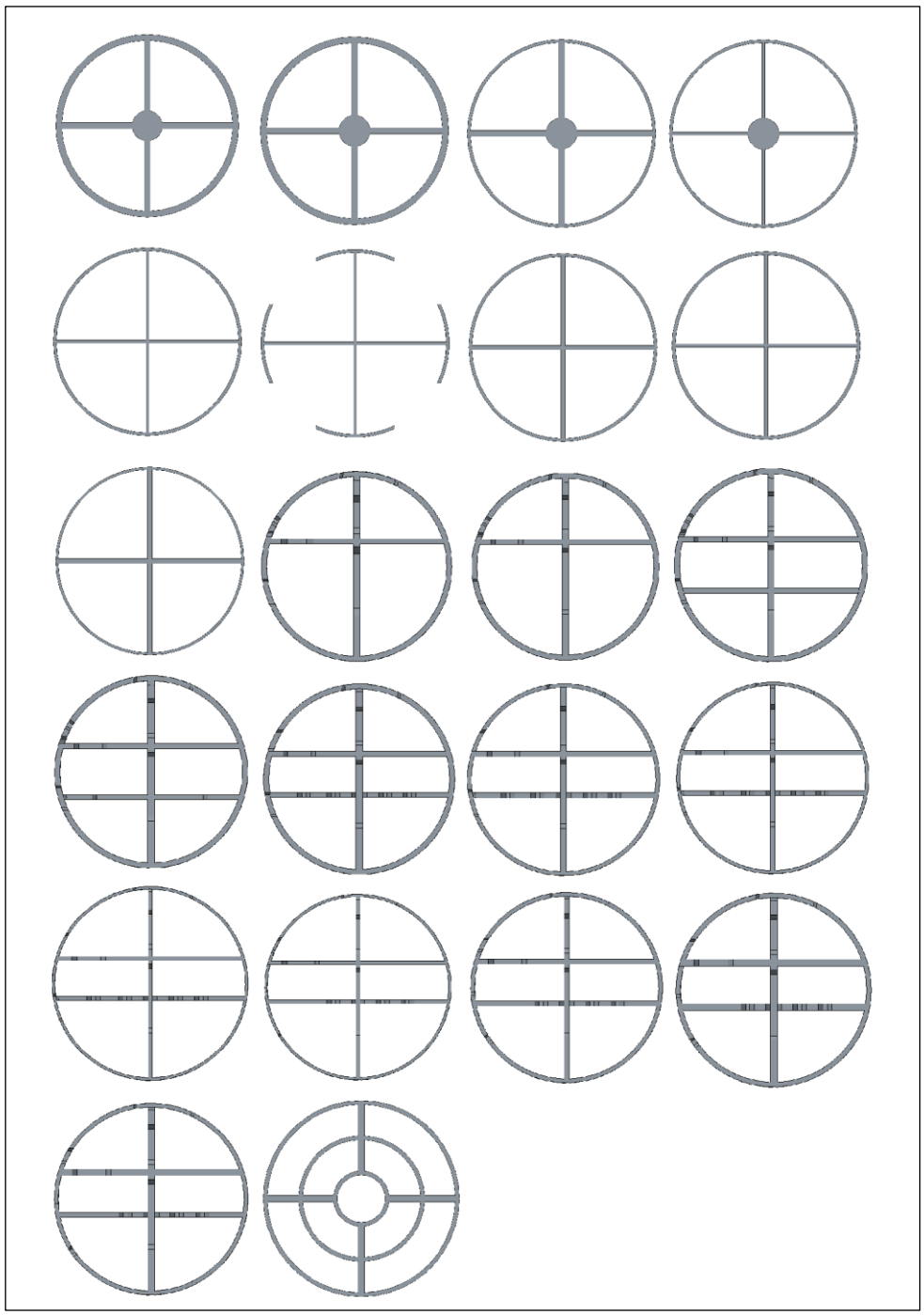

Figure 12
All 22 spacer revisions in order from left to right and top to bottom

The first nine revisions of the spacer design were iterated through to find the optimal dimensions that reduced surface area while still keeping the board deflection under its limit. The main dimensions that were altered are referenced in figure 13. This result was quantified in the last column of table 4 by dividing the difference in surface area from the original design by the difference in deflection from the original design. The more negative this result was, the more the area was decreased for a smaller increase in deflection, so the best result was revision 7. These results are displayed in figure 14.

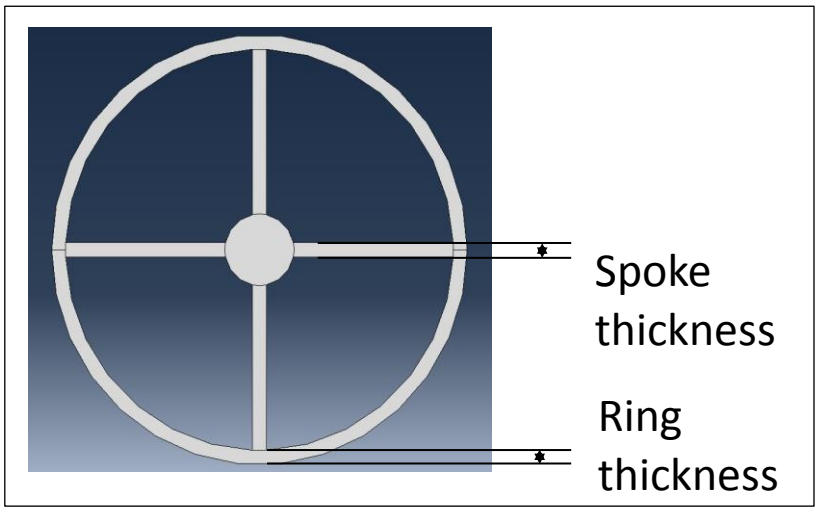

Figure 13
Reference for dimension definitions for revisions 1 through 9

Table 4
First group of iterations geometry and analysis results

Revisions	Spoke thick (inches)	Ring thick (inches)	Deflection (in.*10^3)	Change in deflection	Surface area (in.^2)	Change in surface area	d(area)/d(deflection)
1	0.1	0.1	3.8	0.00	1.57	0.00	0
2	0.1	0.1	7.2	3.37	1.34	-0.23	-0.068
3	0.1	0.05	4.6	0.74	1.14	-0.43	-0.579
4	0.05	0.05	5.2	1.41	0.90	-0.67	-0.474
5	0.05	0.05	5.5	1.70	0.75	-0.82	-0.480
6	0.05	0.05	8.7	4.81	0.55	-1.02	-0.212
7 (best)	0.07	0.05	5.0	1.20	0.86	-0.70	-0.588
8	0.055	0.055	5.3	1.44	0.82	-0.74	-0.517
9	0.08	0.04	5.1	1.30	0.83	-0.74	-0.564

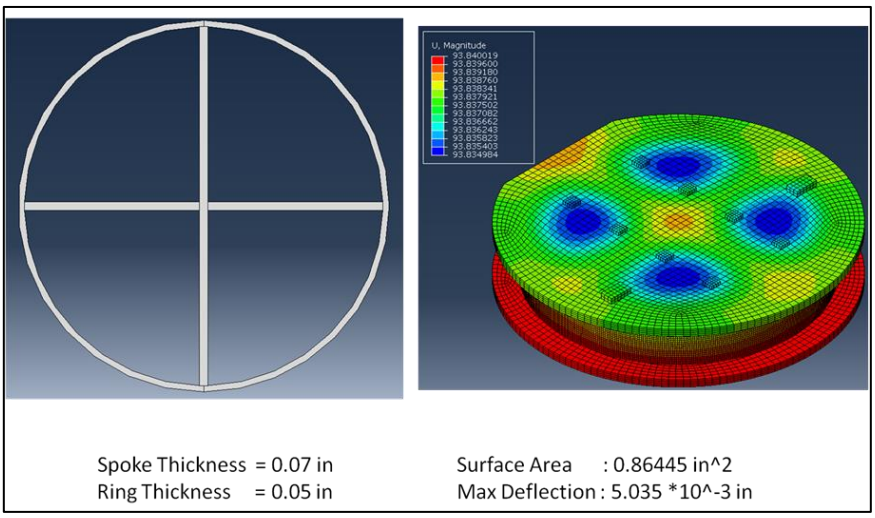

Figure 14
Displacement map of best spacer design (revision 7) in first group of iterations

The second iterating process went through eight revisions in order to fit the spacer over the existing board components without compromising the deflection of the board. This design required moving the spokes of the spacer so that they would interfere with components as little as possible (fig. 15). The metric for the best revision was to find that which reduced deflection for a smaller increase in material. This was done by dividing the difference in volume from revision 10 by the difference in deflection from revision 10. The closer the result was to zero meant that less material needed to be added to reduce the deflection by a larger amount. Table 5 lists the complete set of results for this series of revisions. The best revision found was revision 17, shown in figure 16.

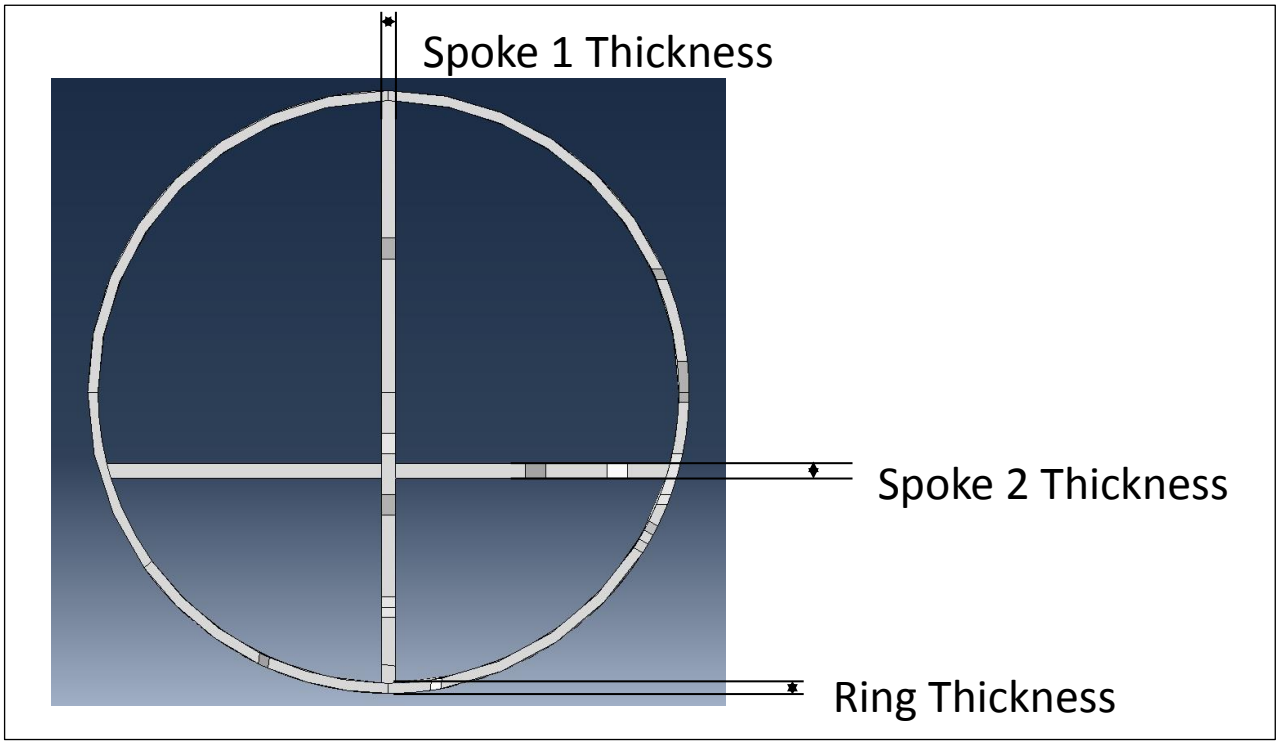

Figure 15
Reference for geometry definitions for revisions 10 through 17

Table 5
Second group of iterations geometry and analysis results

Revisions	Spoke 1 thick (inches)	Spoke 2 thick (inches)	Ring thick (inches)	Deflection (in.*10^3)	Change in deflection	Volume (in.^3)	Change in volume	d(volume)/d(deflection)
10	0.07	0.07	0.05	10.0	0.00	0.389	0.000	0
11	0.08	0.10	0.08	8.3	-1.62	0.567	0.178	-0.110
12	0.08	0.10	0.08	7.9	-2.07	0.655	0.266	-0.129
13	0.08	0.10	0.08	5.3	-4.64	0.661	0.272	-0.059
14	0.08	0.10	0.08	3.6	-6.38	0.669	0.280	-0.044
15	0.08	0.09	0.06	3.9	-6.06	0.579	0.190	-0.031
16	0.07	0.07	0.05	4.4	-5.56	0.489	0.100	-0.018
17 (best)	0.06	0.06	0.04	4.9	-5.04	0.411	0.022	-0.004

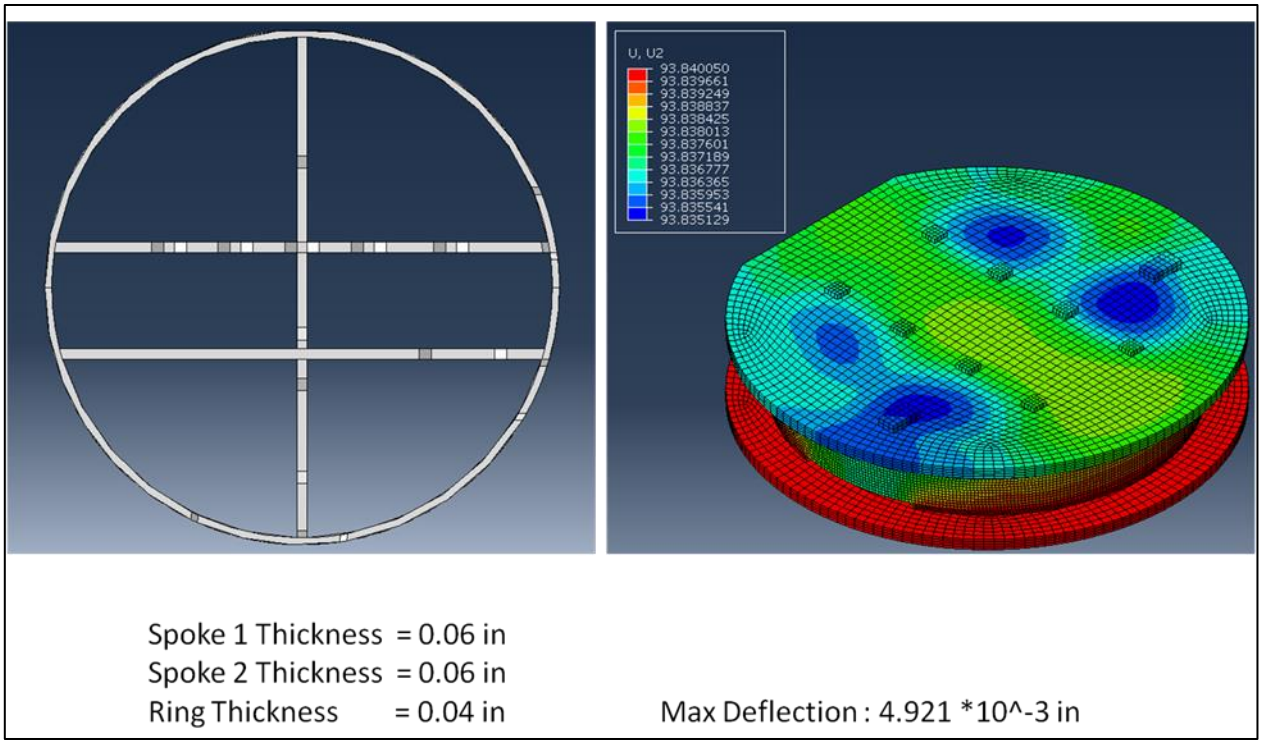

Figure 16
Displacement map of best spacer design (revision 17) in second group of iterations

Revisions 18 through 21 were modifications made after testing the spacer in the full model. The criteria for these was not reducing full board deflection, but rather, reducing the deflection in localized regions across components. Material was added to the spacer for extra support, but this also required cutting away material to leave room for the components. Four more revisions were needed to find this balance.

The final revision of the spacer, shown in figure 17, was intended to provide the most support for the board without taking into account the placement of the components. The intent of this approach was to place the components around the spacer instead of cutting the spacer and reducing its structural integrity. Based on the results of past revisions, the ring of the spacer was most responsible for reducing deflection, so multiple rings were added to magnify this effect. This resulted in a design that used less material than most of the previous revisions, with a much lower deflection.

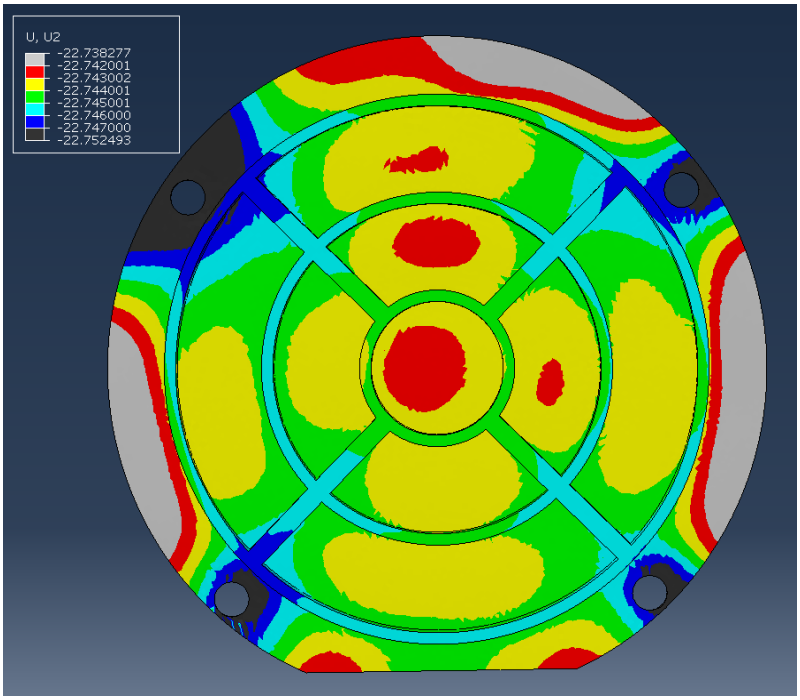

Figure 17
Final revision of spacer with deflection map

Figure 17 can be used as a placement guideline for the components on the boards. Each color represents a differential in deflection of 0.001 in. Therefore, by overlaying this image on top of the board layout, one might measure the deflection across a component through visual inspection.

Initial Method – On-board Recorder Resulting Product

The resulting OBR is shown in figure 18, with the left picture (fig. 18a) of just the board set and the right picture (fig. 18b) showing the stack up with spacers. The spacer fitments are shown in figure 19.

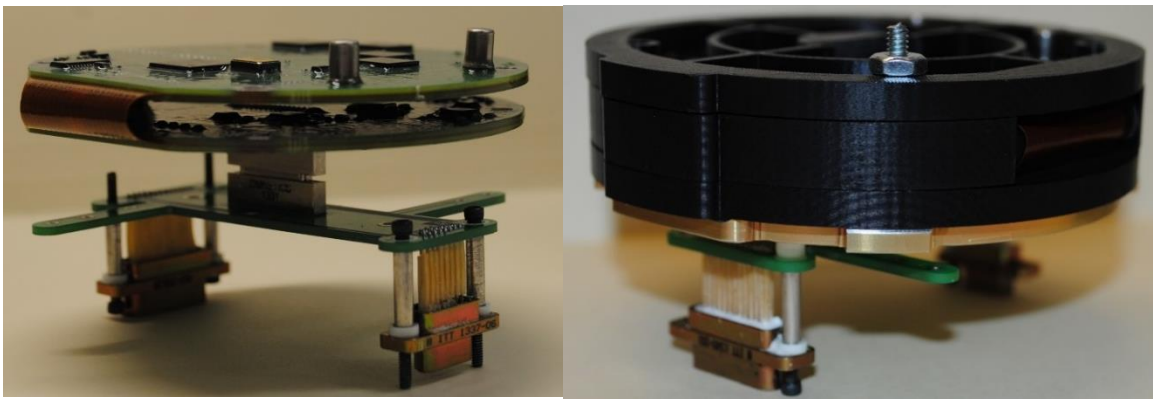

(a)
Board form

(b)
With spacers

Figure 18
Resulting OBR PCB flex assembly

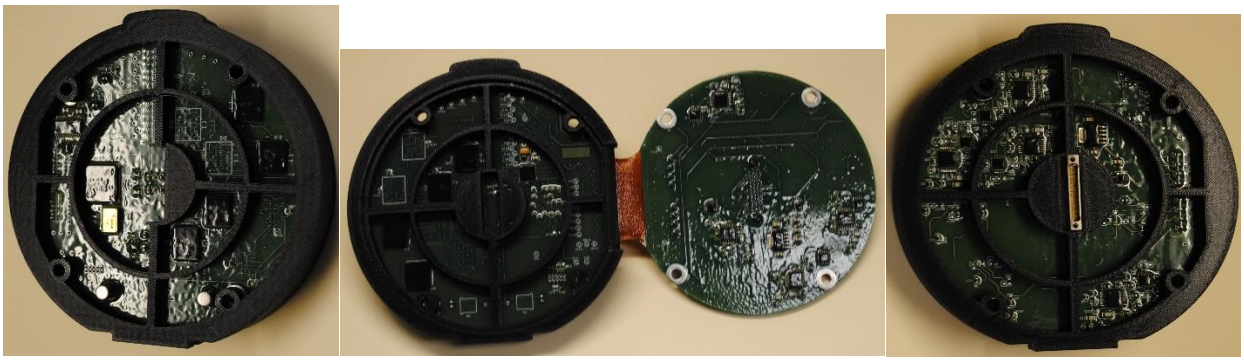

(a) Top (b) Center (c) Bottom

Figure 19
PCB spacers

All components on the PCBs were underfilled using Zymet CN-1533 followed by conformal coating using Miller Stephenson's urethane conformal coat. Two OBRs were built, one with Miller Stephenson MS-470C and the other with Miller Stephenson L0102A. These two materials were not included in the model since the model tied the components to the PCBs, which can be translated to the use of underfill on all components creating an infinitely strong and rigid connection.

At this point of the development, a material change was made from what was originally modeled. A material was selected to match the structural integrity of the polycarbonate used in the FEA models, but that would also allow for three-dimensional (3D) printing of the spacer structures. The acrylonitrile butadiene styrene (ABS)-M30 was used due to its high stiffness and strength, as well as its ability to be printed in 0.005-in. layers. The fine layering of the material allowed for maintaining of the tight tolerances, which allowed for the PCBs to snap into their spacer supports. The 3D printing process also allowed for the quick and cost-effective prototype spacers since traditional computer numerical control machining practices would be cost prohibitive for the features, and an injection molding process development carries a fairly significant initial development time/cost. The detailed characterization of the material properties of 3D printed reinforced plastics is an ongoing effort that still requires further work.

Application of the Initial Method onto a Guidance Electronics Unit (GEU) Board Stack and Comparison between Methods

A comparison was run using another circuit board stack, a GEU board stack, in order to determine the effectiveness of spacers versus potting. Three models were run, as shown in figure 20. A non-potted assembly, but with steel standoffs for maintaining board separation, was used as a control. Another model was run using a set of three ABS-M30 spacers. During the development of this method, the material to be used was switched to ABS-M30 for its ability to print in 0.005-in. layers, and thus allow for tighter tolerance controls, which provide similar stiffness and strength to the polycarbonate. The third model was potted, represented by a single Dolphs CR1050 part surrounding the boards and steel standoffs.

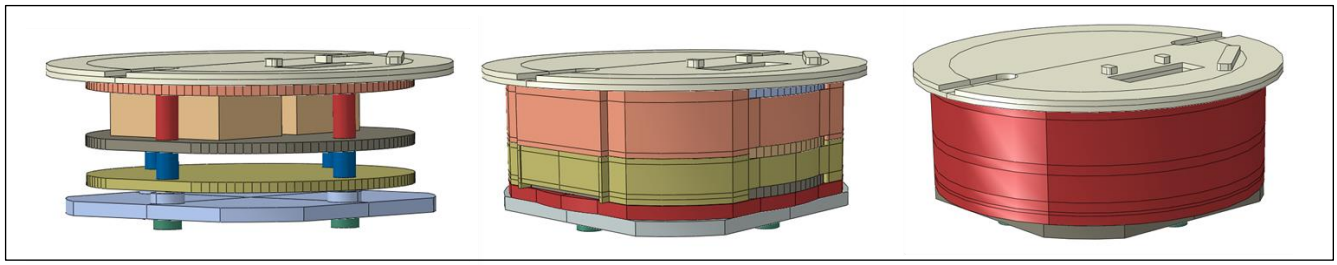

(a)
Unsupported

(b)
Spacers

(c)
Potted

Figure 20
Comparison models

In figure 21, each model was loaded identically using the U.S. Modular Artillery Charge System (MACS) zone 5 acceleration profile. Two constraints were used, one to tie the bolts to the top plate and another to tie the two large components to the boards, as seen in figure 22.

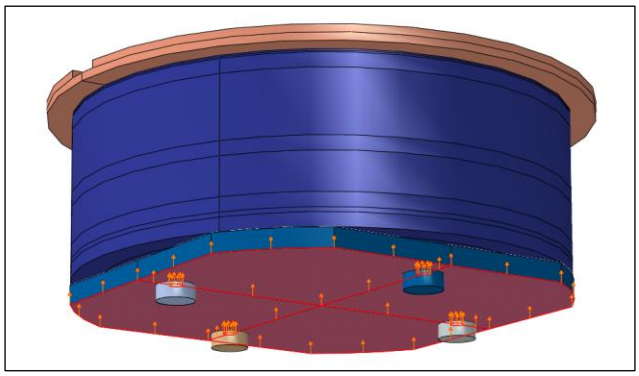

Figure 21
Representative loading shown on potted model

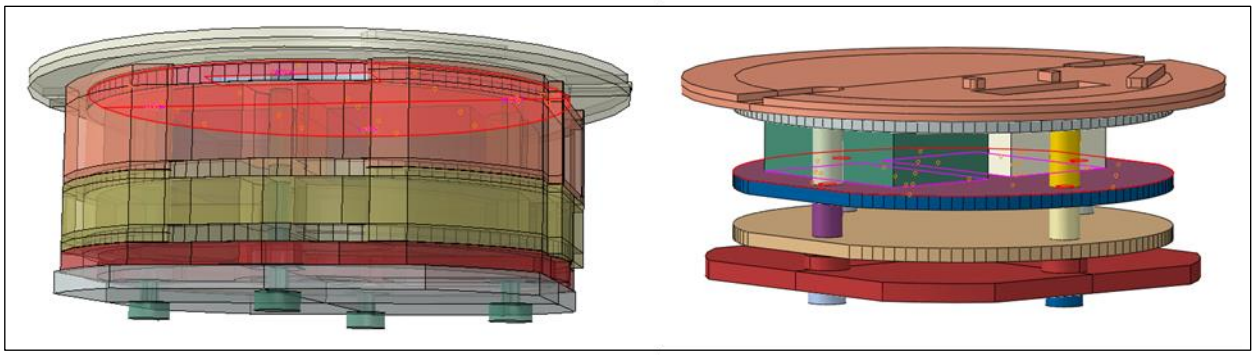

Figure 22
Tie constraints are identical for all three models

The results of these analyses are shown in table 6 in conjunction with figure 23. The spacers performed very close to potting, compared to being unsupported. Potting, as would be expected, provided more support than the other two scenarios. Spacers were still very effective, reducing deflection from 65% up to 78% compared to the unsupported model. It should be noted that the deflections tabulated are total displacements relative to the entire PCB. The previously mentioned

0.005-in. failure criteria is actually intended to be across a single component solder joint, so the tabulated numbers aren't a perfect comparison to PCB failure. They provide a relative understanding of the impact of the structural supports compared to potting. For individual component evaluation, it is useful to apply the contour plots such as figure 17 with the 0.001-in. contour bands to visually see where relative deflections are severe on the PCB relative to the component positioning on the PCB.

Table 6
Boards deflection in thousandths of an inch

Board	Potted	Spacer	Unsupported	Potted/spacer percent reduction
1. Top PCB	1.945	4.109	13.508	85.6/69.6
2. Middle PCB	0.684	5.627	16.120	95.6/65.1
3. Bottom PCB	0.973	3.701	16.709	94.2/77.9

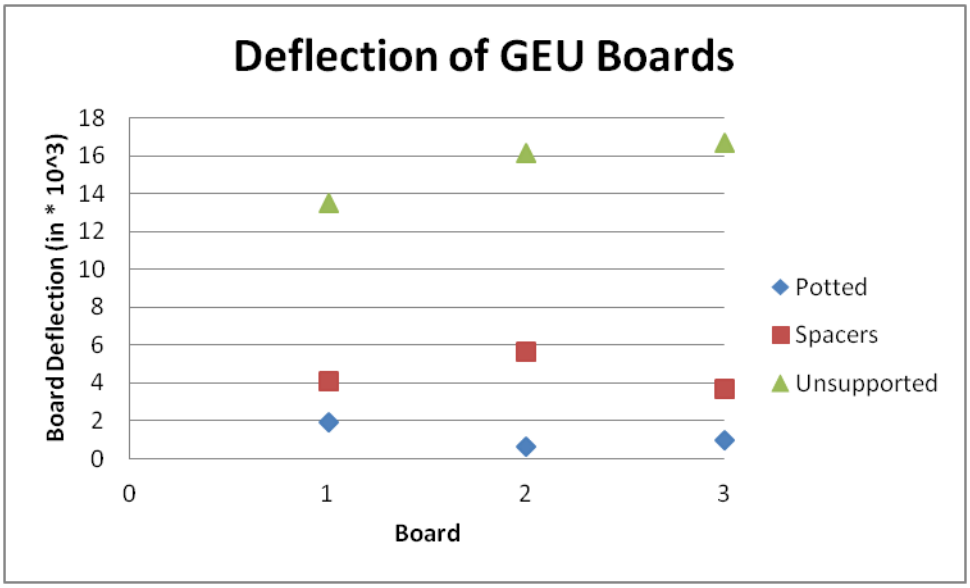

Figure 23
Deflection comparison between the three board stack models

Discussion

This analysis used a simplified model of the projectile assembly during gun launch to determine the deflection of the circuit boards when using spacers instead of potting. The final design of the spacer was such that the maximum deflection of any component on either board was below the amount that designates failure. This shows that the spacer is an acceptable replacement for electronics potting in providing structural support when such a proper design methodology is used for the spacer design and PCB population.

The FEA was used to calculate the board deflection under the prescribed loading conditions. Using this model, the results indicate that the spacer allows the boards to survive gun launch. Many simplifications were made to the model in order to reduce computational time. None of these affect the deflection of the boards in any significant way, so the results obtained should be valid for a physical prototype as well.

Guidance Electronics Unit Resulting Product

Photographs of the GEU board and spacer assembly followed by integration into the housing are shown in figure 24.

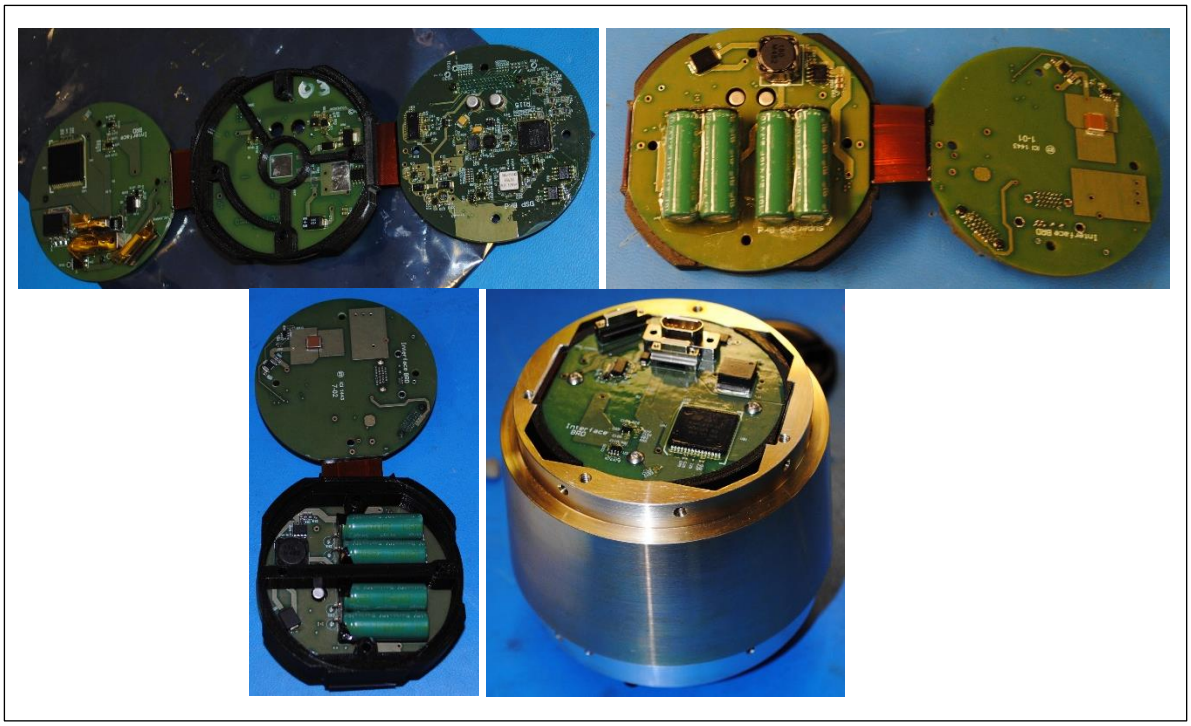

Figure 24
GEU assembly photos

The super capacitors had a fillet of Devcon S-209 epoxy applied to the perimeter and down the center of each super capacitor banks. All other components on the PCBs were underfilled using Zymet CN-1533 followed by conformal coating using Miller Stephenson's urethane conformal coat L0102A. These materials were not included in the model since the model tied all components to the PCBs, which can be translated to the use of underfill on all components (and epoxy on the super caps), creating an infinitely strong and rigid connection.

VALIDATION

The spacer concept has been validated to provide electronics survival capabilities through multiple shots fired from the ARDEC 155-mm Soft Catch Artillery (SCAT) gun. Two separate test events occurred. The axial acceleration data presented was post processed with a 50 kHz digital filter.

Test Event Number One

Present during this test event, SCAT test no. 825, were the spacer OBR with an OBR electronics two board stack that used two spacers (as described previously in this report), as well as an identical OBR with a board set that did not make use of a flex layer between the circuit boards, but instead were wired and soldered together. This unit also used mechanical standoffs for spacing

of the boards in lieu of plastic spacers, and was fully encapsulated in Dolphs CR1050 (this OBR is shown in fig. 25, cross sectioned to illustrate the PCB integration and potting material).

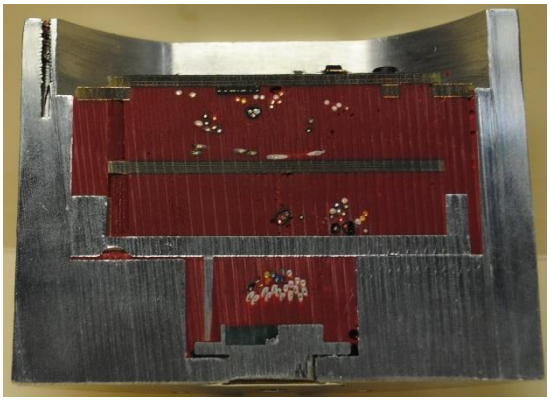

Figure 25
OBR integration cross section

The SCAT test no. 825 was fired at MACS 5 and had a projectile weight of 103.4 and an estimated muzzle velocity of 792.27 m/s. The data of both the spacer OBR and potted OBR are found in figure 26.

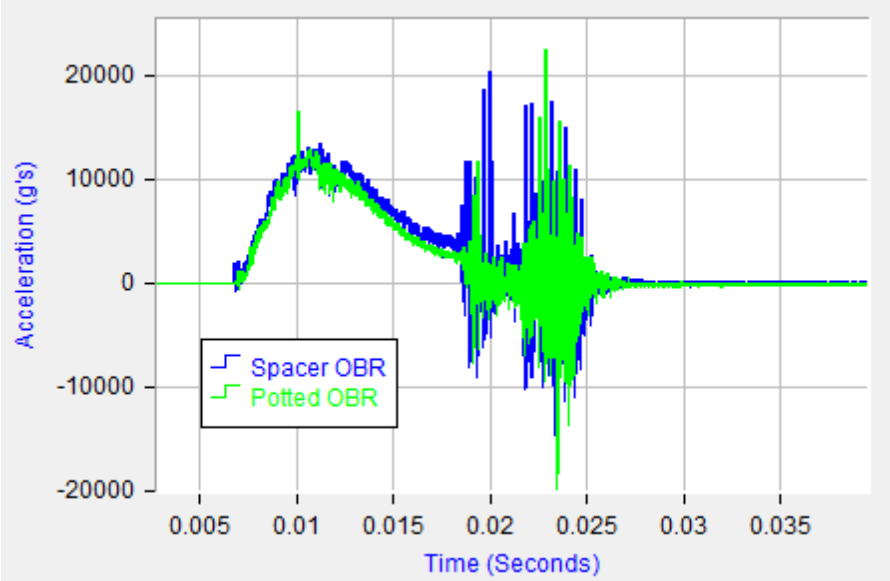

Figure 26
SCAT test no. 825, spacer and potted OBR axial acceleration data

The data recorded on the spacer OBR correlated to that of the potted OBR significantly. Spacer damage was noted in two places: the first location is marked by a broken inner ring on the top spacer, and the second location is noted where one of the innermost supports around the connector separated at its thinnest section (fig. 27). The damage was most likely attributed to the setforward event and insufficient electronics stack preloading within the aluminum housing, shown in figure 27.

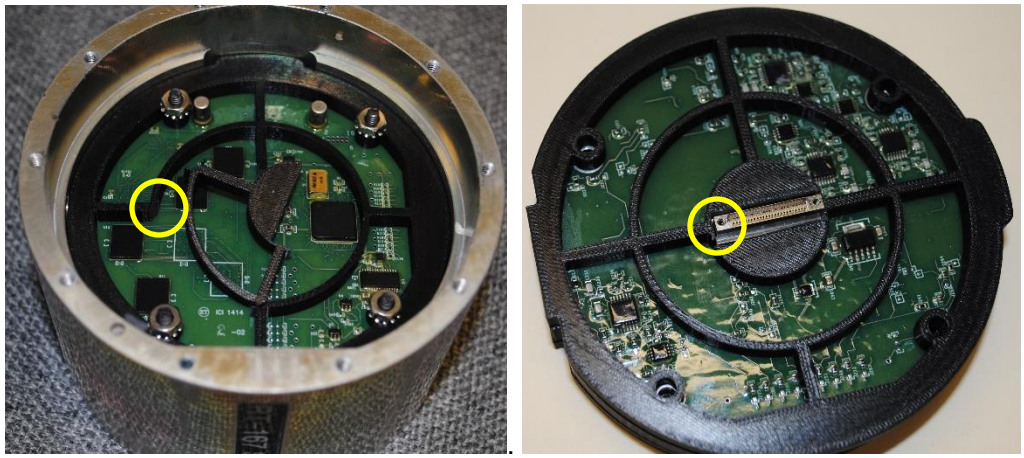

Figure 27
OBR spacer damage

The cracks developed in an area with a sharp edge, as highlighted in the figure. The setforward ringing attributed to the SCAT Gun was not incorporated in the FEA model, so damage due to such had not been predicted. The parts were redesigned as a result to incorporate fillets, and subsequent testing with these fixes has shown reliable survivability. To test the fatigue life of the spacers, multiple shots were fired from the SCAT Gun using spacer OBRs rather than the usual potted OBRs. The intention is to try to identify the weak link in the design through multiple over test events. To the date of this report, the unit has been fired three sequential times without failure.

Test Event Number Two

During this testing event, the validation of the spacer design occurred in the two systems discussed previously: the OBR and GEU. The first shot in this event, SCAT test no. 911, involved shooting both the spacer OBR and potted OBR for continued comparison. The electronics within both OBRs survived SCAT test no. 911 and captured identical data as shown in figure 28.

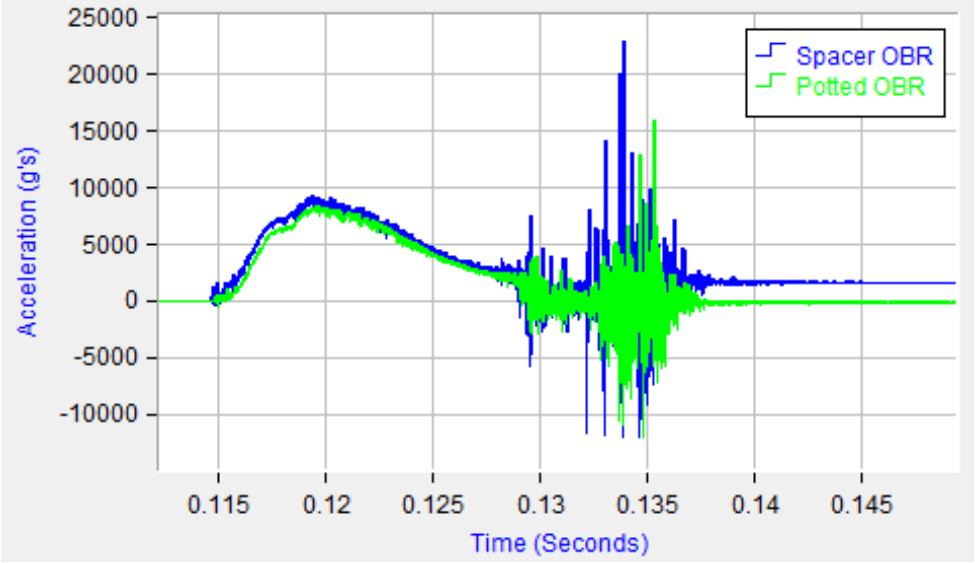

Figure 28
SCAT test no. 911, spacer and potted OBR axial acceleration data

The SCAT test no. 911 was fired at MACS 4, and had a projectile weight of 104.08, with an estimated muzzle velocity of 683 m/s, breech pressure of 32.24 ksi at 4.88 ms, and a chamber pressure of 31.7 ksi.

The spacer OBR was fired two more times, both at MACS 4, with the test parameters shown in table 7 and their axial acceleration curves shown in figure 29.

Table 7
SCAT test nos. 912 and 914 firing parameters

Shot number	Total weight (lb)	Estimated muzzle velocity (m/s)	Breech pressure and rise time	Chamber pressure
912	96.84	701.55	30.4ksi at 4.85 ms	29.9 ksi
914	97.18	698.57	29.99ksi at 4.88 ms	29.69 ksi

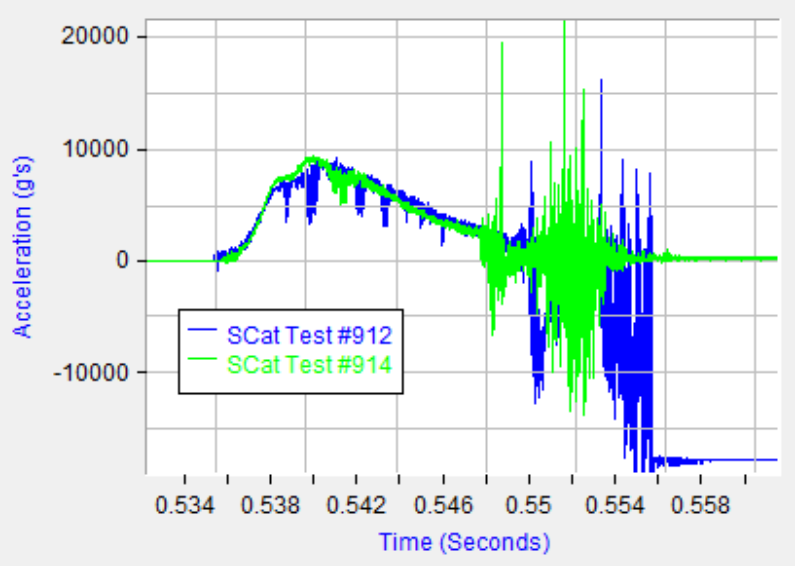

Figure 29
Spacer OBR SCAT test nos. 912 and 914 axial acceleration data

From the data shown in figure 29, the axial acceleration recorded from shot no. 912 was very noisy, had a bias shift occurring after the setforward event, and recorded setforward after that of shot no. 914. By the spacer OBR's next shot, no. 914, the data collected was not as noisy and did not encounter a bias shift. While the schematic and the code were identical between both the spacer OBR and the potted OBR, the differences included: different PCB layout, flexible interconnect over through hole wired connections, and 20,000 g range accelerometer (50 kHz frequency response) that was reused from previous systems instead of the typical 60,000 g range accelerometer (100 kHz frequency response). The 20,000 g range accelerometers are replaced at the first sign of measurement anomalies.

The GEU board stack, inside its housing, was also fired from the SCAT gun unpotted with spacers as supports. After the shot, the boards were tested and deemed to be working perfectly, with no electrical abnormalities, and as of the date of this report, remains to be the primary electronics development board set for its program. The damage to the stack was restricted to a small indentation in a spacer where a connector terminal pin protruded from the underside of its PCB. Otherwise, the boards and spacers appeared undamaged, looking exactly as they did before the shot.

CONCLUSIONS

Based on the results of these analyses, the final spacer design is a feasible alternative to the more traditional method of electronics potting. This spacer can be used instead of potting in order to allow for more flexibility in adjusting the electronics components. It also avoids making contact with components, reducing the risk of failure from stresses induced through thermal expansion. Using a spacer instead of potting in a computer-aided engineering model will reduce complexity and allow for faster modeling and analysis.

REFERENCES

1. Berman, M.S., “Electronic Components for High-g Hardened Packaging,” Technical Report ARL-TR-3705, Aberdeen Proving Ground, Aberdeen, MD, January 2006.

2. Chao, N.H., DeAngelis, M., Lee, J., Kleinbach, K.S., and Cheng, R.B., “Advanced Modeling for Miniaturized Potted Smart Munitions Development,” in ASME 2013 International Design Engineering Technical Conference and Computers and Information in Engineering, Portland, OR, August, 2013.

3. Chao, N.H., Dispenza, J.A., and DeAngelis, M.E., “Advanced Methodologies for Developing Improved Potted Smart Munitions for High-G Applications,” ASME "Journal of Electronic Packaging," vol. 135, no. 3, September 2013.

4. Chao, N.H., Carlucci, D., Cordes, J.A., DeAngelis M.E., and Lee, J., “Implication of a Fully-Coupled Thermal Stress Transient Simulation in Gun-Lunch Applications,” Technical Report ARMET-TR-10030, U.S. Army ARDEC, Picatinny Arsenal, NJ, November 2010.

5. Chao, N.H., Cordes, J., Carlucci, D., DeAngelis, M.E., Marhevka, S., Lee, J., Reinhardt, L., and Tesla, M., “The Use of Potting Materials for Electronic-Packaging Survivability in Smart Munitions,” in Proceedings of the 2010 International Mechanical Engineering Conference and Exposition, IMECE2010-37433, Vancouver, BC, November, 2010.

6. Haynes, A., Cordes J.A., and Krug, J., “Thermomechnical Impact of Polyrethane Potting on Gun Launched Electronics,” Journal of Engineering, vol. 2013, p. 11, September 2012.

7. Cordes, J., Geissler, D., Mougeotte, C., Lowe, R., Foley, J., Ganguli, S., Ferguson, J., and Roy, A., “Modeling and Simulation of Circuit Boards with Resistors, Subjected to Multiple High-G Loads,” Technical Report ARMET-TR-14029, U.S. Army ARDEC, Picatinny Arsenal, NJ, November 2014.

8. Geissler, D., Mougeotte, C., Cordes, J., Lowe, R., Foley, J., and Dodson, C., “Numerical Assessment of Modeling and Simulation of Electrical Components,” Technical Report ARMET-TR-13068, U.S. Army ARDEC, Picatinny Arsenal, NJ, September 2014.

9. Cordes, J., Lee, J., Myers, T.L., Hader, G., Reinhardt, L., Kessler, C., Gray, N., and Guevara, M.A., “Statistical Comparisons Between Qualification Tests for Gun-Fired Projectiles,” Journal of Applied Mechanics, vol. 77, pp. 051602-1 - 051602-6, September 2010.

10. Adolf, D., Spangler, S., Austin, K., Neidigk, M., Neilsen, M., and Chambers, R., “Packaging Strategies for Printed Circuit Board Components Volume I: Materials & Thermal Stresses,” Sandia Report SAND2011-4751, Sandia National Laboratories, Albuquerque, NM, September 2011.

11. Stout, C., Terhune, R., Carlucci P., and Mougeotte, C., “Failure Analysis of a 105mm Fin Deployment Mechanism,” Proceedings of the 2010 Simulia Customer Conference, May, 2010.

DISTRIBUTION LIST

U.S. Army ARDEC
ATTN: RDAR-EIK
RDAR-MEF-E, S. Manole
C. Stout
N. Baldwin
R. Granitzki
J. Caplinger
D. Weinhold
A. Rotundo
Picatinny Arsenal, NJ 07806-5000

Defense Technical Information Center (DTIC)
ATTN: Accessions Division
8725 John J. Kingman Road, Ste, 0944
Fort Belvoir, VA 22060-6218

GIDEP Operations Center
P.O. Box 8000
Corona, CA 91718-8000
gidep@gidep.org

REVIEW AND APPROVAL OF ARDEC TECHNICAL REPORTS

Method for Designing Electronic Assemblies
Title Without Potting for Gun Launched Applications Through the Use of Additive Manufacturing — Date received by LCSD

Steven Manole
Author/Project Engineer — Report number (to be assigned by LCSD)

x2744 — 94 — RDAR-MEF-E
Extension — Building — Author's/Project Engineers Office (Division, Laboratory, Symbol)

PART 1. **Must be signed before the report can be edited.**

a. The draft copy of this report has been reviewed for technical accuracy and is approved for editing.

b. Use Distribution Statement A X, B ___, C ___, D ___, E ___, F ___ or X ___ for the reason checked on the continuation of this form. Reason: _____

1. If Statement A is selected, the report will be released to the National Technical Information Service (NTIS) for sale to the general public. Only unclassified reports whose distribution is not limited or controlled in any way are released to NTIS.

2. If Statement B, C, D, E, F, or X is selected, the report will be released to the Defense Technical Information Center (DTIC) which will limit distribution according to the conditions indicated in the statement.

c. The distribution list for this report has been reviewed for accuracy and completeness.

Douglas C. Troast — 2 Feb 2016
Division Chief — (Date)

PART 2. To be signed either when draft report is submitted or after review of reproduction copy.

This report is approved for publication.

Douglas C. Troast — 3 Feb 16
Division Chief — (Date)

Andrew Pskowski — 12/15/16
RDAR-CIS — (Date)

LCSD 49 supersedes SMCAR Form 49, 20 Dec 06